Nanoelectromechanical systems

M. P. BLENCOWE*

Department of Physics and Astronomy, 6127 Wilder Laboratory, Dartmouth College, Hanover, NH 03755, USA

Nanoelectromechanical systems (NEMS) are nano-to-micrometer scale mechanical resonators coupled to electronic devices of similar dimensions. NEMS show promise for fast, ultrasensitive force microscopy and for deepening our understanding of how classical dynamics arises by approximation to quantum dynamics. This article begins with a survey of NEMS and then describes certain aspects of their classical dynamics. In particular, we show that for weak coupling the action of the electronic device on the mechanical resonator can be effectively that of a thermal bath, this despite the device being a driven, far-from-equilibrium system.

1. Introduction

A nanoelectromechanical system (NEMS) consists of a nanometer-to-micrometer (micron) scale mechanical resonator that is coupled to an electronic device of comparable dimensions [1–6]. The mechanical resonator may have a simple geometry, such as a cantilever (suspended beam clamped at one end) or a bridge (suspended beam clamped at both ends) and is fashioned out of materials such as silicon using similar lithographic techniques to those employed for fabricating integrated circuits. Because of their (sub)micron size, the mechanical resonators can vibrate at frequencies ranging from a few megahertz (MHz) up to around a gigahertz (GHz) [7,8]; we are not normally accustomed to the idea of mechanical systems vibrating at such high radio-to-microwave frequencies.

The coupling to the electronic device can be achieved electrostatically by applying a voltage to a metal film deposited on the surface of the mechanical resonator. One example of a coupled electronic device is a single electron transistor (SET) shown in figure 1. Electrons quantum tunnel one at a time across the transistor from drain electrode to source electrode, driven by a drain-source voltage V_{ds} (we adopt the usual convention where positive charges flow from source electrode to drain electrode and hence negative charges flow the opposite way). The magnitude of the resulting current depends on another voltage applied to a third, gate electrode, called the gate voltage V_g. With the metallized mechanical resonator forming part of the gate electrode, motion of the former will modulate the gate voltage and hence the drain-source tunnelling current, which is subsequently amplified and detected.

With the high frequencies and small inertial masses of the nanomechanical resonators, together with the ultrasensitive mechanical displacement detection capabilities of the coupled electronic devices, NEMS show great promise for metrology. One possible area of application is force microscopy, where a cantilever tip is scanned over a surface and the cantilever displacements measured as the tip interacts with the surface used to build up a force topography map. Of particular interest is the magnetic resonance force microscope (MRFM) which employs a ferromagnetic cantilever tip, enabling the mapping of unpaired electron and nuclear spin densities at and below the surface [10]. Recently, single electron spin detection sensitivities were achieved [11,12]; the potential applications of being able to determine chemical identity at the single molecule or atom level are numerous. And with the use of smaller, suitably-engineered NEMS MRFM devices, the higher mechanical frequencies might result in faster read-out times at equivalent or better sensitivities.

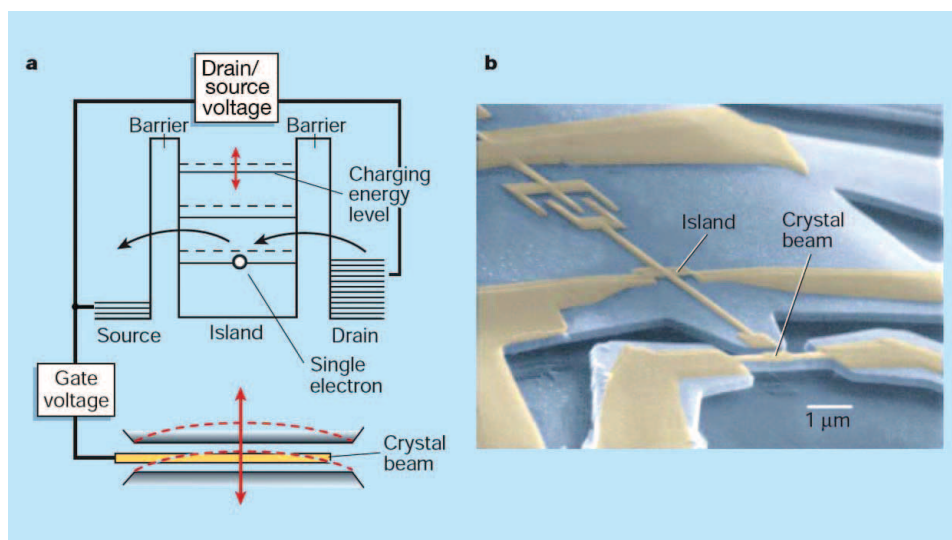*Corresponding author. Email: Miles.P.Blencowe@Dartmouth.EDU

M. P. Blencowe

Figure 1. (*a*) Cartoon illustrating the operation of the SET displacement detector. The indicated charging energy levels represent the energy cost arising from the change in stored electric field energy as one or more electrons tunnel onto the island; the discreteness of the levels are not a quantum effect, but rather the incremental energy cost to put increasing numbers of electrons on the island at the same time. (*b*) False-coloured scanning electron microscope (SEM) micrograph showing the suspended, doubly-clamped beam and SET [9]. The substrate and beam are fashioned from GaAs (blue regions), and the SET and beam gate electrodes are thin layers of aluminum (yellow regions), with aluminum oxide forming the tunnel barriers. The beam is located 0.25 μm away from the island electrode. The measured fundamental flexural frequency for in-plane motion is about 116 MHz.

Another application is mass-sensing, where the mass of a small particle attaching itself to a nanomechanical resonator can be determined from the resulting vibrational frequency-shift of the resonator. Recently, attogram ('atto' $\equiv 10^{-18}$) detection sensitivities were achieved [13,14]. With the use of suitably-engineered higher frequency NEMS, the detection of individual molecules may be possible at single-Dalton sensitivities (1 Dalton = 1.66×10^{-27} kg, 1/12 the mass of a C^{12} atom) [15].

NEMS can be interesting in their own right as nontrivial dynamical systems. Because of the small inertial mass of the nanomechanical resonator and the strong electrostatic coupling to the closely integrated electronic device that can be achieved, individual electrons travelling through the latter can give significant displacement 'kicks' to the mechanical resonator. In turn, the motion of the resonator will influence the electron current and so on. At cryogenic temperatures, certain electronic devices can behave in a quantum coherent fashion, existing in a quantum superposition of different charge states as electrons are transmitted through the device. Interacting with such a device, the mechanical resonator's centre-of-mass may be driven into a quantum state [6], such as a superposition of separated position states. The quantum nature of the coupled electromechanical system will manifest itself in certain signatures of the measured current. Nanomechani-

cal resonators comprise up to about ten billion atoms, so that by most standards such quantum effects would be deemed macroscopic. It is important to appreciate that we are here referring to quantum effects in 'dirty real' devices that possess both many electronic and mechanical degrees of freedom, and which interact strongly with the surrounding environment consisting of photons, phonons, fluctuating (charged) defects in both the mechanical resonator and electronic device etc. The experimental and theoretical investigation of such systems will lead to a deeper understanding of how classical dynamics emerges as an approximation to quantum dynamics; NEMS straddle the microscopic quantum and macroscopic classical worlds.

In the first generation of experiments to probe the dynamics of NEMS (see, e.g. [9,16–21]), the mechanical resonator component has been found to behave classically, as might be expected; the experiments are not yet quite refined enough to observe quantum interference effects that are washed-out by the resonator's environment. Despite this, the (semi)classical dynamics of NEMS has been found to be nontrivial and worthy of investigation. One line of investigation is to identify common features in the classical dynamics of the various NEM devices, so as to bring some degree of coherence to the field. Remarkably, under certain conditions of weak coupling and also wide separation of mechanical and electronic dynamical time-scales, the

electronic device behaves effectively as a thermal bath: the mechanical resonator undergoes thermal brownian motion, characterized by a damping constant and effective temperature which are determined by the electronic parameters of the device [22,23]. The fact that the electronic device can be effectively replaced by a thermal bath is at first sight rather surprising, given that the voltage-driven electron current flowing through the device is a far-from-equilibrium, many electron state. The use of well-understood equilibrium concepts in the construction of theoretical models of less-well-understood non-equilibrium systems goes back to the early days of statistical mechanics and continues to find broad application. For a recent review, see for example [24].

The outline of this article is as follows: section 2 gives examples of various representative NEM devices that are being investigated. Section 3 analyses the classical dynamics of the SET-mechanical resonator system, focusing on the effective equilibrium description in the weak-coupling regime. Section 4 describes the effective equilibrium dynamics of some of the other NEMS introduced in section 2. Section 5 gives concluding remarks.

2. Survey of NEMS

In this section we describe several representative NEMS. The explanations as to how they work will be qualitative and brief in nature, centering on schematic diagrams or electron microscope images of each device.

Figure 2 shows a schematic diagram of a mechanically compliant tunnelling electrode taken from [25]. The tunnelling electrode consists of a cantilever with metal tip which is placed close to the surface of a bulk metal counterelectrode. As is common in theoretical analyses of NEMS, the cantilever is simply modelled as a harmonic

oscillator with some effective spring constant and mass. Electrons tunnelling across the gap between the metal tip and surface cause the cantilever to recoil, while in turn the cantilever's motion affects the electron tunnelling probability and hence the measured tunnelling current. Thus, we have a coupled electromechanical system which should display some interesting dynamical properties, depending on the applied voltage across the gap, gap size, cantilever's mass, spring constant etc. There have been several theoretical investigations of the mechanical tunnelling electrode and related schemes [22,25 – 32]. In a sense, the scanning tunnelling microscope [33] is an experimental realisation, since a tunnelling electrode cannot be made absolutely rigid. However, a device with a deliberately compliant, low-mass tunnelling electrode, such that the tunnelling electrons themselves cause significant recoil of the electrode, has yet to be demonstrated.

Figure 3 shows a scanning electron microscope (SEM) micrograph of a quantum point contact (QPC) displacement detector developed by Andrew Cleland's group at UC Santa Barbara [34]. The detector comprises a suspended beam etched from a single-crystal gallium arsenide (GaAs) heterostructure with a fundamental resonance frequency for out-of-plane flexural motion of about 1.5 MHz. Within the beam is a thin layer of free electrons, called a two-dimensional electron gas, (see, e.g. [35] for an elementary review of 2DEG and other low-dimensional semiconductor systems) which forms a current when a drain-source voltage is applied across the ends of the beam. Applying also a sufficiently negative voltage to the metal gate electrodes on
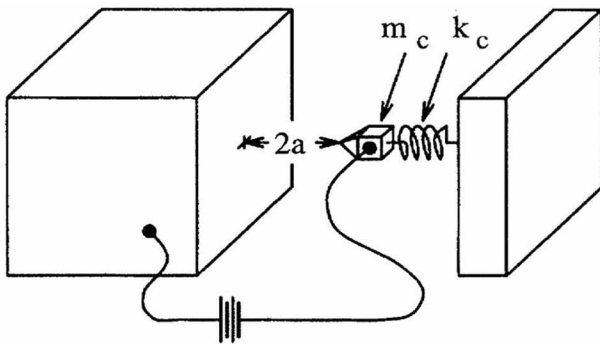

Figure 2. Scheme for a mechanically compliant tunnelling electrode [25]. The cantilever electrode is modelled as a harmonic oscillator with some spring constant κ_c and mass m_c. A voltage is applied across the gap $2a$ and the resulting current measured.
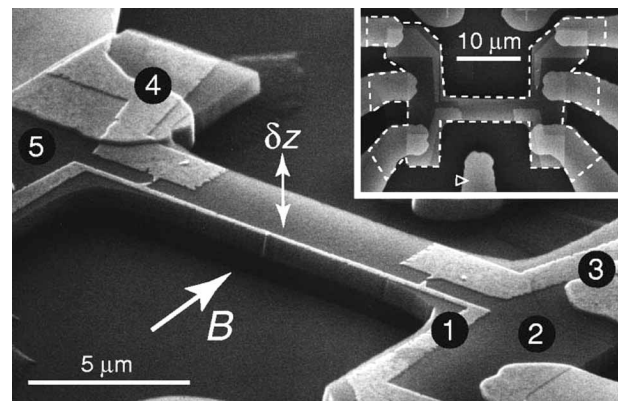

Figure 3. SEM micrograph of QPC displacement detector, showing the suspended beam with electrodes on the surface [34]. The gate electrodes are labelled '1' and '3'. The point contacts forming the narrow constriction are located just above label '1'. The drain and source electrodes are labelled '5' and '2'. The indicated magnetic field is used to actuate the beam; the Lorentz force on the electron current causes flexing displacements in the indicated z direction.

the surface of the beam expels the electrons from directly beneath the elecrodes so that they can only flow through the narrow, electrostatically defined constriction between the point contacts. The constriction can be made narrow enough such that it is comparable to the electrons' Fermi wavelength; hence the name 'quantum point contact'. Because GaAs is a piezoelectric material, mechanical strain in the flexing beam will induce a polarization electric field in the beam. This induced polarization field has the same effect as applying a gate voltage, hence modulating the current flowing through the QPC. In turn, the fluctuating electric field due to the flowing current will induce a mechanical strain. Thus, the QPC displacement detector is another example of a coupled electromechanical system.

Figures 1, 4, and 5 show various realisations of the single electron transistor (SET) displacement detector. The device in figure 1 was developed by Cleland's group [9,16], while the device in figure 4 was developed by Keith Schwab's group at the Laboratory for Physical Sciences, U Maryland [17,18]. Figure 5 shows a scheme being developed by Herre van der Zant's group at Delft [36]. The latter device differs from the first two in that the SET island is mechanically-compliant instead of the gate electrode. A closely-related transistor device integrating a suspended carbon nanotube was recently demonstrated by Paul McEuen's group at Cornell [20]. The basic operating principle of the SET displacement detector is illustrated in figure 1(*a*). The source and drain aluminum electrodes are electrically insulated from the island electrode by an oxide layer. However, because the oxide layer is very thin, electrons can quantum tunnel across the oxide barriers, from drain-to-island-to-source, constituting a current which is measured after subsequent amplification stages. In order for an electron to be able to tunnel from, e.g. the drain to the island electrode, the total work done by the drain-source
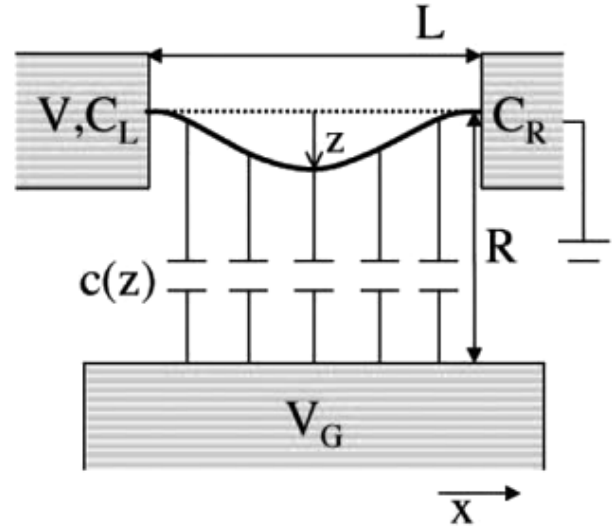

Figure 5. Scheme for a SET with mechanically-compliant island formed out of a suspended carbon nanotube [36]. As a result of the electrostatic coupling between the voltage-biased gate and island, the position of the latter fluctuates as electrons tunnel on and off.
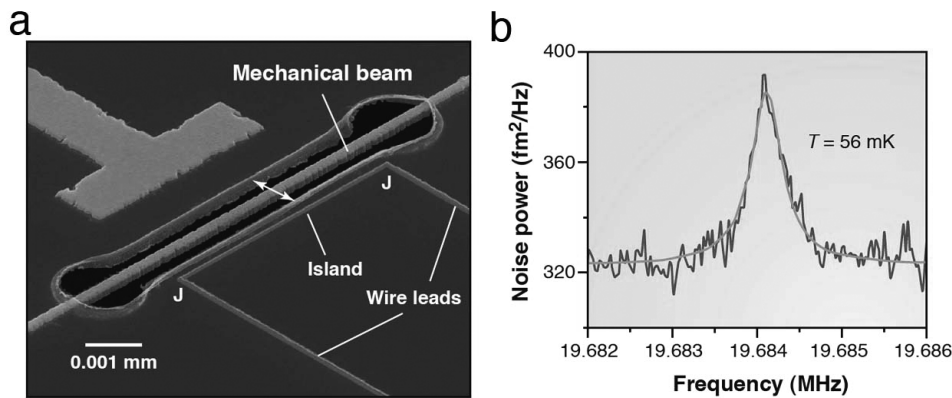

Figure 4. (*a*) SEM micrograph showing the mechanical beam and SET drain-source wire leads and island [17]. Electrons tunnel one at a time across the electrically-insulating junctions located at the corners (J). The beam and surrounding substrate are fashioned from a silicon-nitride (SiN) membrane, a commonly-used material for NEMS because of its high strength-to-mass density ratio. The beam is coated with a layer of gold, forming the gate electrode, while the SET island and leads are made from aluminum. The mechanical resonator is located 0.6 μm away from the island. The large, fixed gate electrode at the upper left is used for displacement actuation. (*b*) SET-detected noise power spectrum converted to displacements-squared. The Lorentzian peak due to the mechanical beam's thermal brownian motion is clearly seen above the amplifier noise background. The measured fundamental frequency for in-plane motion is about 19.7 MHz.

and gate voltages must exceed the accompanying change in the stored electric field energy due to the redistribution of the charges on the various electrodes (called the 'charging energy'); the difference between the work done and the charging energy gives the net energy gained by the tunnelling electron, which must be positive. Because of the small sizes of the electrodes, their mutual capacitances are small and so the charging energy is large. Hence, a large enough drain-source voltage must be applied in order to meet this charging energy cost so that electrons can tunnel through the device. If, however, the voltage is not large enough to overcome the charging energy required to put more than one electron simultaneously on the island, then only one electron can tunnel on and off the island at a time (hence the name 'single electron transistor').

The charging energy can be offset by the applied gate voltage, so that varying the gate voltage modulates the tunnelling current. Alternatively, by applying a fixed voltage to the mechanically-compliant beam gate electrode, motion of the latter will also modulate the tunnelling current. Figure 4(*b*) shows an example from Schwab's group of the SET-detected signal of the mechanical beam undergoing thermal brownian motion. The area under the peak after subtracting off the white-noise background (which mostly originates from the subsequent amplification stages) gives a root-mean-squared displacement of about 2×10^{-13} m, with a position detection sensitivity set by the white-noise floor of about 10^{-13} m. To put these numbers into perspective, this SET is able to detect displacements as small as one-thousandth the diameter of a hydrogen atom. Furthermore, such sensitivities are within an order of magnitude of the quantum zero-point displacement uncertainty of the mechanical beam.

Using the classical equipartition of mechanical energy for a harmonic oscillator, $\langle E \rangle = m\omega^2 \langle x^2 \rangle = k_B T$, it is possible to directly determine the temperature of the mechanical beam from the measured mean-squared displacement, resonant frequency and effective motional mass (which can be estimated from the beam dimensions and mass density). The data in figure 4(*b*) corresponds to a beam temperature of about 60 mK. This value sets a record for the lowest directly measured temperature of a nanomechanical resonator. The actual, base temperature of the refrigerator is about 35 mK, suggesting that there is some local heating of the beam. Most likely, the energy released by the tunnelling electrons in the SET is not dissipating quickly enough.

In addition to heating the mechanical beam resonator, the tunnelling electrons will directly influence the motion of the resonator: the fluctuating island voltage due to electrons tunnelling on and off the island will produce a back reaction force on the electrostatically coupled resonator. The magnitude of this force noise increases with applied gate voltage. The displacement detection sensitivity also increases, so that there is an optimum gate voltage bias point which is neither too large nor too small. On the other hand, if our interest is not in displacement detection, but rather the investigation of the coupled dynamics of NEMS, then the gate voltage should be increased beyond this optimum bias point so that there is a large back reaction on the resonator . Motion of the resonator then modulates the tunnelling current and in turn the fluctuating current drives the mechanical resonator. Experiments are underway in Schwab's group to explore the coupled dynamics in this back reaction-dominated regime.

Figure 6 shows a nanomechanical charge shuttle developed by Dominik Scheible at Ludwig Maximilians University, Munich, and Robert Blick at the University of Wisconsin [19]. The mechanical shuttle element is a nanopillar fashioned out of silicon with a conducting island at the top made out of gold. An ac voltage is applied to the source electrode at a frequency close to the fundamental flexural frequency of the pillar. When there is an excess charge on the island, the ac voltage exerts a force on the pillar, driving it into mechanical oscillation at the ac frequency. If the ac voltage amplitude is sufficiently large, then the shuttle will deflect close enough to the source and drain electrodes such that electrons can tunnel between the island and the electrodes. The pillar then shuttles charge between the two electrodes, producing a current that is detected at the drain electrode. The number of electrons that tunnel and the tunnel direction depend on the magnitude and sign of the drive voltage at the instant of closest approach to a given electrode, i.e. on the phase lag
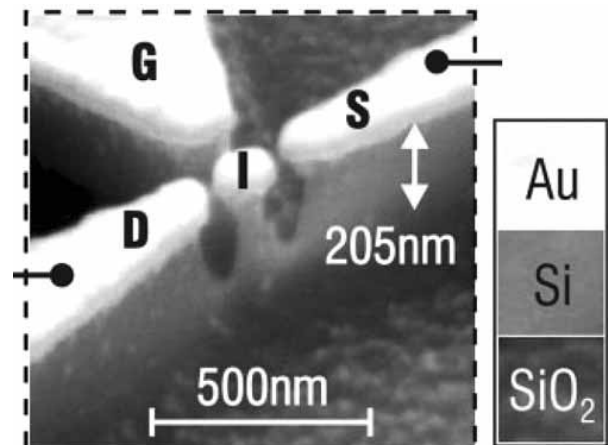

Figure 6. SEM micrograph of the silicon nanopillar with gold island (I) and source (S) and drain (D) electrodes [19]. The gate (G) electrode was not used in the experiment. The current is detected from the drain electrode after amplification. The nanopillar has a fundamental flexural frequency of 367 MHz.

between the oscillating mechanical motion and drive voltage. The phase lag in turn depends on the drive frequency relative to the fundamental frequency of the shuttle. Thus, the magnitude and direction of the shuttle current can be controlled by varying the drive frequency. The charge shuttle bears some resemblance to the SET with mechanically compliant island shown in figure 5. However, as the name implies, in contrast to the above-described NEM devices mechanical motion of the shuttle is essential for an electron current to flow; the electronic and mechanical degrees of freedom are inextricably linked in their dynamics. Shekhter *et al.* [37] gives a review of charge shuttle systems.

In this section, we have introduced several examples of NEM devices. The following sections will explore certain aspects of their coupled dynamics, with a central goal being to identify commonalities in their dynamical behaviour. In this respect, it will be useful to view a NEM device according to the generic scheme of figure 7. The mechanical resonator, which will be simply modelled in its lowest fundamental vibrational mode as a harmonic oscillator, is an open system that is coupled to two energy reservoirs. The electronic device through which an electron current flows constitutes one of the reservoirs where the current exchanges energy with the oscillator via the electromagnetic interaction. All degrees of freedom apart from those of the electronic device and the oscillator constitute the second, 'external' reservoir. These degrees of freedom consist, for example, of higher vibrational modes, fluctuating defects etc. within the mechanical resonator and air molecules, photons etc. impinging the surface of the resonator. These external degrees of freedom are simply modelled as one infinitely large thermal equilibrium bath at some temperature T_{ext}. If the oscillator is initially in an excited state, then in the absence of the electronic device it will lose energy to this bath at a rate which can be expressed as ω/Q_{ext}, where ω is the oscillator frequency and Q_{ext} is the quality factor. Nanomechanical resonators are typically found to have quality factors between $10^3 - 10^5$ [3], so that a resonator oscillates at least a few thousand cycles before its amplitude has substantially decayed from the initial excited amplitude.

We shall pay particular attention to the dynamics of the oscillator system as a result of its interactions with these two reservoirs. In this respect, we shall envisage a separate, idealized direct probe of the oscillator dynamics allowing perfect measurement of its position and velocity coordinates without affecting its dynamics. In actual NEMS experiments, information about the mechanical resonator dynamics is obtained by measuring the electron current: the electronic device is after all usually intended as a displacement detector. For some theoretical investigations about how the dynamics of the mechanical resonator manifests itself in the current signal output, see, e.g. [30,38–42].
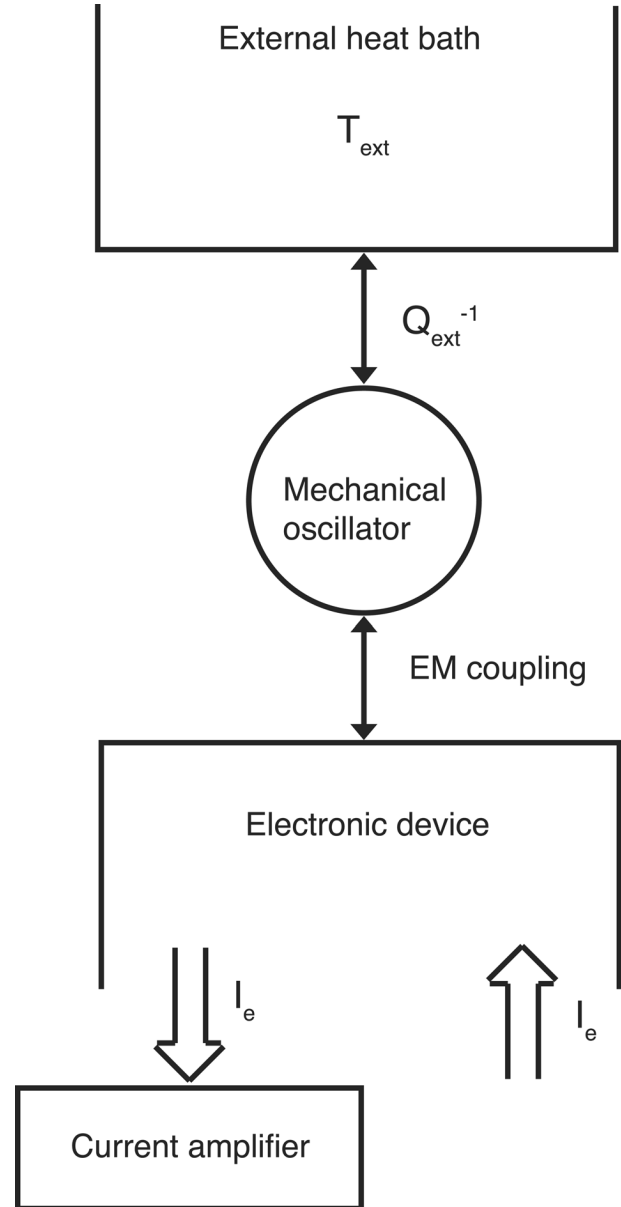

Figure 7. Scheme of a generic NEMS.

3. The SET-nanomechanical resonator system

In this section we describe the coupled classical dynamics of the SET-mechanical resonator system. The coupled dynamics of other NEMS will be considered in section 4. Referring to the generic scheme of figure 7, we shall in the first instance omit the coupling to the external thermal bath (i.e. $Q_{\text{ext}} \to \infty$); we are interested in elucidating the 'pure', coupled dynamics of the oscillator interacting with the SET only. For example, is this system stable in the sense that the tunnelling electron current removes energy from an initially excited oscillator causing damping, or do the tunnelling

electrons dump energy into the oscillator driving it to progressively larger amplitudes? The answer is not obvious a priori.

3.1 *The master equation*

We seek some form of manageable equation of motion which describes the SET-mechanical resonator system. The logical starting point is the time-dependent Schrödinger equation with Hamiltonian involving the relevant microscopic degrees of freedom, in particular the conduction electrons in the various SET electrodes, and the fundamental oscillator mode (recall we are neglecting for the time being the external environment of the oscillator mode). One then proceeds through various stages of approximation to arrive at simpler-to-handle classical statistical equations of motion along with some conditions for their validity. However, for NEMS at least, this procedure still needs to be properly developed and is essential to the future goal to achieve a deeper understanding of how classical dynamics emerges from quantum dynamics by approximation in these systems.

In the absence of such a properly-defined procedure, we shall instead use physical intuition to guide us directly towards writing down the classical statistical equations of motion. There is a long tradition employing such an approach going back to Boltzmann and his famous equation. One advantage is that such equations often accurately capture the statistical dynamics as verified by experiment. Another particular advantage in our case is that the dynamics in the regime of strong electromechanical coupling is easier to analyze than in the full quantum theory. The general disadvantage is that the precise conditions for the validity of the classical equations of motion are not available, with the consequence that important terms can occasionally be overlooked. This is believed not to be a problem for the SET-oscillator classical equations which we shall shortly write down.

What minimal set of coordinates is required to describe the mechanical resonator interacting with the SET? Modelled as a single oscillator mode, the resonator's state is described by a position x and velocity v coordinate. With respect to the oscillator, the relevant SET coordinate is the total number N of excess electrons on its island; depending on N, the electrostatic force will pull the oscillator towards the island by different amounts. (If we were to also describe the SET drain-source current, we would need an additional counter coordinate which keeps track of the number of electrons entering (or leaving) the SET). Because tunnelling is a random process, the coordinates N, x and v will fluctuate. Thus, the equations of motion can either take the form of stochastic differential equations involving the random, time-varying functions $N(t)$, $x(t)$ and $v(t)$ (see e.g. [43] for an introduction on how to describe stochastic

processes), or we can write down a deterministic equation involving the probability density function $P_N(x,v,t)$. In the latter formulation, $P_N(x,v,t)dxdv$ is interpreted as the probability at time t of picking out from a large number of identical SET-oscillator systems (an ensemble), one system with island number N and with position and velocity coordinates in the respective intervals $[x,x + dx]$ and $[v,v + dv]$. We shall choose to express the dynamics in terms of the probability density function, rather than in terms of stochastic coordinates. Referring to the circuit diagram for the coupled SET-resonator system (figure 8), we have [23]

$$\frac{\partial P_N}{\partial t} = \{H_N, P_N\} - \left(\Gamma_L^- + \Gamma_R^+\right)P_N + \left(\Gamma_L^+ + \Gamma_R^-\right)P_{N+1}, \quad (1)$$

$$\frac{\partial P_{N+1}}{\partial t} = \{H_{N+1}, P_{N+1}\} - \left(\Gamma_L^+ + \Gamma_R^-\right)P_{N+1} + \left(\Gamma_L^- + \Gamma_R^+\right)P_N, \quad (2)$$

where $H_{N(N+1)}$ is the oscillator Hamiltonian for the resonator in the background electrostatic potential of the
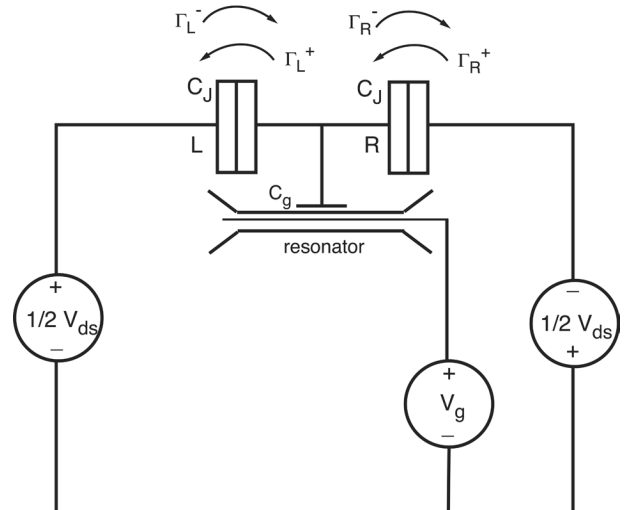

Figure 8. Circuit diagram of the SET-mechanical resonator system. The capacitances of the left (L) and right (R) tunnel junctions are assumed identical, denoted as C_J. The gate capacitance formed by the adjacent resonator and island electrodes is denoted C_g. As the resonator flexes, the distance between the two electrodes varies, hence changing C_g. With the resonator electrode kept fixed at the gate voltage V_g, the changing C_g gives rise to a varying island potential, hence modulating the tunnelling current. For the indicated drain-source voltage (V_{ds}) polarity, the usual direction for electron flow is from right to left, governed by the tunnel rates Γ_R^+ and Γ_L^+.

SET with $N(N + 1)$ electrons on the island, $\{\cdot,\cdot\}$ is the Poisson bracket:

$$\{H_N, P_N\} = \frac{\partial H_N}{\partial x}\frac{1}{m}\frac{\partial P_N}{\partial v} - \frac{1}{m}\frac{\partial H_N}{\partial v}\frac{\partial P_N}{\partial x},$$

and $\Gamma^{\pm}_{L(R)}$ are the electron tunnelling rates to the left ($+$) or to the right ($-$) across the left (L) or right (R) tunnel junctions. Here, we are assuming that the voltages are chosen such that the number of excess electrons on the island fluctuates between N and $N + 1$ only.

Equations (1) and (2) describing the evolution of the probability distribution $P_{N(N + 1)}(x,v,t)$ are commonly called 'master equations'. They are coupled, first-order partial differential equations in the variables x, v and t. Once an initial probability distribution has been specified, then these equations uniquely determine the subsequently evolving probability distribution. For example, the distribution at some initial time t_0 might take the form $P_N(x,v,t_0) = \delta(x)\delta(v)$ and $P_{N+1}(x,v,t_0) = 0$, meaning that at time t_0 all SET-oscillator systems within the ensemble are in the same state, with the oscillator's position and velocity being $x = 0$ and $v = 0$, respectively, and the SET island number being N. If the tunnelling rate terms were absent in equations (1) and (2) then the evolving probability distribution would remain a delta function, describing deterministic harmonic oscillator motion with the island number remaining fixed at N. Choosing the origin of the coordinate x to coincide with the equilibrium position of the oscillator when there are N electrons on the island, the oscillator Hamiltonians take the form

$$H_N = \frac{p^2}{2m} + \frac{1}{2}m\omega^2 x^2 \tag{3}$$

$$H_{N+1} = \frac{p^2}{2m} + \frac{1}{2}m\omega^2(x - x_0)^2, \tag{4}$$

where x_0 is the distance between equilibrium positions of the oscillator with N and $N + 1$ electrons on the island. With the tunnelling rate terms present, however, the evolving probability distribution begins to spread. The fluctuating electron island number due to electrons tunnelling on and off the island causes the deterministic evolution of the oscillator to be interrupted at random times by a sudden shift $\pm x_0$ in the origin of the harmonic potential experienced by the oscillator.

The placings and the signs in front of the various tunnelling rate terms in the master equations (1) and (2) are easily understood from figure 8. For example, in equation (1), the first two rates Γ^-_L and Γ^+_R correspond to tunnelling onto the island and so decrease the likelihood that the island number remains at N; hence the 'minus' sign. On the other hand, the second two rates Γ^+_L and Γ^-_R correspond to

tunnelling off the island and so increase the likelihood that the island number becomes N; hence the 'plus' sign. The tunnelling rates can be derived using Fermi's Golden Rule [44] and take the form

$$\Gamma^{\pm}_{L(R)} = \frac{1}{e^2 R_J}\frac{E^{\pm}_{L(R)}}{1 - e^{-E^{\pm}_{L(R)}/k_B T_e}}, \tag{5}$$

where R_J is the effective tunnel junction resistance (assumed the same for each junction), T_e is the temperature of the source, drain and island electron reservoirs (assumed the same) and $E^{\pm}_{L(R)}$ is the energy gained by a single electron tunnelling to the left ($+$) or to the right ($-$) across the left (L) or right (R) junction. When the electron temperature T_e is small compared to the single electron charging energy, i.e. $k_B T_e << e^2/2C_\Sigma$ (where the total SET capacitance is $C_\Sigma = 2C_J + C_g$), then equation (5) becomes approximately

$$\Gamma^{\pm}_{L(R)} = \frac{1}{e^2 R_J}E^{\pm}_{L(R)}\Theta(E^{\pm}_{L(R)}), \tag{6}$$

where $\Theta(\cdot)$ is the Heaviside step function. Thus, a given tunnel rate is only non-negligible provided the associated E is positive. For micron-scale SETs, $C_\Sigma \sim 1\text{fF}(\equiv 10^{-15}\text{ F})$, giving $T_e << 1\text{K}$. In most experiments, this condition is satisfied and so from now on we will use expression (6) for the rates. For the indicated drain-source voltage polarity in figure 8, rates Γ^+_R and Γ^+_L describing tunnelling to the left are non-negligible, while the rates Γ^-_R and Γ^-_L for tunnelling to the right are exponentially suppressed. Note, however, that through the E's, the tunnel rates also depend on the oscillator's position x; it is possible that, for large enough amplitude displacements and applied gate voltages, a given E changes sign hence switching on or off the corresponding tunnel process and changing the tunnelling direction.

The above master equation pair (1) and (2) is clearly classical. The probability distribution characterizes the classical statistical uncertainty in ones knowledge of the precise coordinates x, v of the oscillator and island electron number. The equations do not entertain the possibility of quantum superpositions between different island number states, different oscillator position/velocity states, or entangled oscillator-island states. Quantum mechanics only enters in the determination of the effective tunnel junction resistances R_J appearing in the rate expressions (5), essentially providing the randomness of the transition rates. Refering to the discussion at the beginning of this section, the classical master equation can in principle be derived from the Schrödinger equation describing the time-evolution of the density matrix characterising the quantum state of the harmonic oscillator and conduction electrons in the SET electrodes. One step in the derivation is to 'trace-out' the many electron state, leaving in the SET state description just the total island number. This step

introduces irreversibility into the equations, as manifested by the tunnelling rate terms. The two key approximation steps out of which a classical description emerges are (1) assume a large enough SET island such that electron energy level quantization can be neglected; (2) assume large enough tunnel junction resistances such that the electron tunnels incoherently between the drain/source and island electrodes. Another approximation step that is made is to assume that the timescale for polarization charges on the electrode surfaces to re-equilibrate in response to a tunnelling event is negligible as compared with the characteristic time between tunnel events given by $\tau_{\text{tunnel}} = eR_J/V_{\text{ds}}$. This is reflected in the fact that the rate of change of the probability densities at time t in the master equation are governed by transition rates that are weighted by probability densities at the same time t and not at earlier times. This is called the 'Markovian' approximation. With the oscillator excluded, the above master equation arising from the various just-described approximations often goes by the name of the SET 'orthodox model' (see, e.g. chapter 4 of [45] for an accessible discussion).

3.2 *The steady state solution*

In solving the master equations (1) and (2), we will first determine the steady state behaviour for $t \to \infty$. Assuming sufficiently large V_{ds} and sufficiently weak coupling between the oscillator and SET such that the energy terms E_R^+ and E_L^+ are always positive, then we need only consider the rates Γ_R^+ and Γ_L^+ as defined in equations (6) with the step function omitted. It is convenient to express the master equations in terms of dimensionless coordinates, since in dimensionless form the essential parameters governing the dynamics are more clearly expressed. Expressing the time coordinate in tunnelling time units τ_{tunnel}, the position coordinate in shift units x_0 and the velocity coordinate in units x_0/τ_{tunnel}, the master equations take the form

$$\frac{\partial P_N}{\partial t} = \varepsilon^2 x \frac{\partial P_N}{\partial v} - v \frac{\partial P_N}{\partial x} + \tilde{E}_L^+ P_{N+1} - \tilde{E}_R^+ P_N, \quad (7)$$

$$\frac{\partial P_{N+1}}{\partial t} = \varepsilon^2 (x-1) \frac{\partial P_{N+1}}{\partial v} - v \frac{\partial P_{N+1}}{\partial x} - \tilde{E}_L^+ P_{N+1} + \tilde{E}_R^+ P_N, \quad (8)$$

where the dimensionless parameter $\varepsilon = \omega \tau_{\text{tunnel}}$ characterizes the separation between the oscillator and SET dynamics timescales. The dimensionless energy terms are obtained by dividing $E_{L(R)}^+$ by eV_{ds}:

$$\tilde{E}_L^+ = -\frac{e}{C_\Sigma V_{\text{ds}}} (N_g - N - 1/2) - \kappa N + 1/2 - \kappa x \quad (9)$$

$$\tilde{E}_R^+ = +\frac{e}{C_\Sigma V_{\text{ds}}} (N_g - N - 1/2) + \kappa N + 1/2 + \kappa x, \quad (10)$$

where $N_g = C_g V_g/e$ is the polarization charge induced by the gate voltage and the dimensionless parameter $\kappa = m\omega^2 x_0^2/(eV_{\text{ds}})$ characterizes the coupling strength between the oscillator and the SET. The shift coordinate has the explicit form $x_0 = -eN_g/(C_\Sigma m\omega^2 d)$, where d is resonator-island electrode gap, so that the coupling strength can be controlled by varying the gate voltage V_g; in particular, κ depends quadratically on V_g. As we shall see, parameters ε and κ are key to describing the coupled SET-oscillator dynamics.

From (7) and (8), we can derive equations for the various moments $\langle x^n v^m \rangle_{N(N+1)}$ of the probability distribution, where

$$\langle x^n v^m \rangle_{N(N+1)} = \int \mathrm{d}x \int \mathrm{d}v x^n v^m P_{N(N+1)}(x, v, t).$$

Solving for the moments is a more manageable task than trying to solve for the full probability distribution all at once. The equations for the moments are

$$\frac{\mathrm{d}\langle x^n v^m \rangle_N}{\mathrm{d}t} = -m\varepsilon^2 \langle x^{n+1} v^{m-1} \rangle_N + n\langle x^{n-1} v^{m+1} \rangle_N + E_L \langle x^n v^m \rangle_{N+1} \\ - E_R \langle x^n v^m \rangle_N - \kappa \left(\langle x^{n+1} v^m \rangle_N + \langle x^{n+1} v^m \rangle_{N+1} \right) \quad (11)$$

$$\frac{\mathrm{d}\langle x^n v^m \rangle_{N+1}}{\mathrm{d}t} = -m\varepsilon^2 \left(\langle x^{n+1} v^{m-1} \rangle_{N+1} - \langle x^n v^{m-1} \rangle_{N+1} \right) \\ + n\langle x^{n-1} v^{m+1} \rangle_{N+1} \\ - E_L \langle x^n v^m \rangle_{N+1} + E_R \langle x^n v^m \rangle_N \\ + \kappa \left(\langle x^{n+1} v^m \rangle_N + \langle x^{n+1} v^m \rangle_{N+1} \right), \quad (12)$$

where the κ-dependent coupling terms have been pulled outside the energy E terms and the '$\sim$' and '$+$' symbols on the latter have been dropped for notational convenience. If the SET damps the oscillator, then in the limit $t \to \infty$ the various moments approach constant values. Thus, we seek a possible solution to (11) and (12) with $\mathrm{d}\langle x^n v^m \rangle_{N(N+1)}/\mathrm{d}t = 0$. Fortunately, these equations can be solved exactly for the time-independent moments. For $n + m = 0,1$, we find [23]

$$\langle x \rangle_{N+1} = \langle P \rangle_{N+1} = 1 - \langle P \rangle_N = \frac{E_R}{1 - \kappa} \quad (13)$$

and $\langle x \rangle_N = \langle v \rangle_N = \langle v \rangle_{N+1} = 0$. For $n + m = 2$, we find for the variances [23]

$$\delta x^2 = \langle x^2 \rangle - \langle x \rangle^2 = \frac{eV_{\text{ds}}}{m\omega^2} \langle P \rangle_N \langle P \rangle_{N+1} \quad (14)$$

258 *M. P. Blencowe*

$$\delta v^2 = \langle v^2 \rangle = (1 - \kappa)\frac{eV_{ds}}{m}\langle P \rangle_N \langle P \rangle_{N+1} \qquad (15)$$

and $\langle xv \rangle_N = \langle xv \rangle_{N+1} = 0$, where the averaged probabilities are defined as

$$\langle P \rangle_{N(N+1)} = \int du \int dv P_{N(N+1)}(x, v, t)$$

and we have returned to the original, dimensionful coordinates.

What can we learn from these solutions to the first few moments? For $\kappa < 1$, the very existence of the solutions is evidence that the SET damps the oscillator, bringing it to a steady state. For $\kappa > 1$ on the other hand, the solutions are ill-defined (note that δv^2, $P_{N+1} < 0$ if $\kappa > 1$) suggesting that the coupled SET-oscillator system may be unstable in this regime. It is not possible to say anything more definite than this about the behaviour in the large κ regime, however, since the approximations to the master equation made above (in particular the omission of the step functions and the tunnelling rates to the right) break down when κ is not small. Note from (14) and (15) that the position and velocity variances are related as

$$\omega_R^2 \delta x^2 = \delta v^2 = \frac{eV_{ds}}{m}\langle P \rangle_N \langle P \rangle_{N+1}, \qquad (16)$$

where the renormalized oscillator frequency is $\omega_R = \sqrt{1 - \kappa}\,\omega$. Now recall that for a classical damped harmonic oscillator in contact with a thermal bath at temperature T, we have equipartition of energy: $\frac{1}{2}m\delta v^2 = \frac{1}{2}m\omega_R^2\delta x^2 = \frac{1}{2}k_B T$. Comparing with equation (16), this suggests that we can assign an effective temperature T_{SET} to the SET given by

$$k_B T_{SET} = eV_{ds}\langle P \rangle_N \langle P \rangle_{N+1}. \qquad (17)$$

Further evidence that the SET behaves effectively as a thermal bath comes from examining the higher moments with $n + m = 3,4....$ For $\kappa << 1$, it is found that the higher moments can be approximately decomposed into products of the lowest moments with $n + m = 1,2$, i.e. $\langle x \rangle$, $\langle x^2 \rangle$, and $\langle v^2 \rangle$. This means that the steady state probability distribution $P(x,v)$ [$= P_N(x,v) + P_{N+1}(x,v)$] for the oscillator is given by a Gaussian to a good approximation, as is the Maxwell-Boltzmann distribution describing a classical harmonic oscillator in contact with a thermal bath:

$$P(x,v) = \frac{2\pi k_B T}{m\omega}\exp\left\{-\frac{m}{2k_B T}\left[\omega^2(x - \langle x \rangle)^2 + v^2\right]\right\}. \qquad (18)$$

Figure 9 shows an example steady-state probability distribution for $P(x)[= \int dv P(x,v)]$ obtained by numerically solving the full master equations (1) and (2) with parameter choices $\varepsilon = 0.3$ and $\kappa = 0.1$. Also plotted is the Gaussian distribution obtained after integrating (18) over the velocity coordinate, with the steady state average position coordinate given by $\langle x \rangle = x_0\langle P_{N+1} \rangle$ [the dimensionful form of equation (13)] and the temperature given by equation (17). As can be clearly seen, the steady state distribution is closely approximated by the Gaussian distribution fixed using the analytically-derived effective temperature and steady state average position coordinate.

3.3 *Mechanical resonator dynamics in the weak coupling regime*

In the previous section, we found that for weak coupling ($\kappa << 1$) the SET appears to the oscillator in the steady state as a thermal bath with effective temperature $k_B T_{SET} = eV_{ds}\langle P \rangle_N \langle P \rangle_{N+1}$. Suppose now that the resonator is not in a steady state, e.g. it is given some initial displacement amplitude and released, undergoing subsequent non-steady state motion. Does the SET still appear to the oscillator as a thermal bath? The following analysis addresses this question and as we shall learn, the SET indeed behaves as a bath, provided there is a wide separation in the oscillator and SET dynamics timescales ($\varepsilon << 1$) in addition to weak coupling.

We seek some approximate way to solve the dimensionless master equations (7) and (8) which takes advantage of the weak coupling condition $\kappa << 1$. The solution should furthermore be a good approximation for times much longer than the oscillator period $2\pi/\omega$ in order to establish
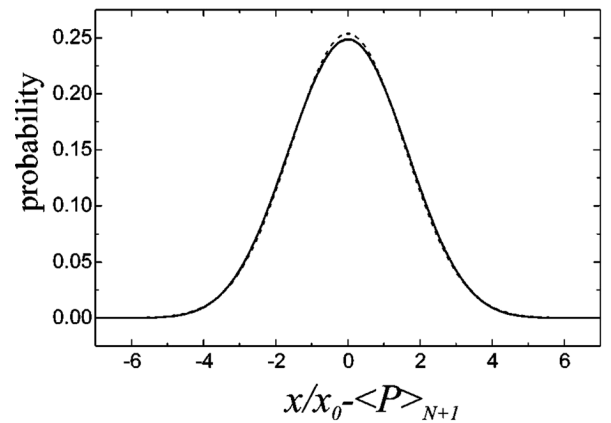

Figure 9. Steady state probability distribution $P(x)$ for $\varepsilon = 0.3$ and $\kappa = 0.1$ [23]. The horizontal coordinates are in units of the shift x_0 and with origin at the steady state average position $x_0\langle P_{N+1} \rangle$. The numerical solution is given by the solid line and the Gaussian fit is the dashed line.

that the SET damps the oscillator. The obvious procedure is to solve for the evolving probability distribution perturbatively using κ as the small expansion parameter. Let us first put the master equations in the following concise, matrix form:

$$\frac{\partial \mathcal{P}}{\partial t} = (\mathcal{H}_0 + \mathcal{V})\mathcal{P}, \tag{19}$$

where

$$\mathcal{P} = \begin{pmatrix} P_N(x,v,t) \\ P_{N+1}(x,v,t) \end{pmatrix},$$

$$\mathcal{H}_0 = \begin{pmatrix} \varepsilon^2 x \frac{\partial}{\partial v} - v \frac{\partial}{\partial x} & 0 \\ 0 & \varepsilon^2 x \frac{\partial}{\partial v} - v \frac{\partial}{\partial x} \end{pmatrix} \tag{20}$$

$$+ \begin{pmatrix} -E_R - \kappa\langle x\rangle & E_L - \kappa\langle x\rangle \\ E_R + \kappa\langle x\rangle & -E_L + \kappa\langle x\rangle \end{pmatrix}$$

and $\mathcal{V} = \mathcal{V}_1 + \mathcal{V}_2$, with

$$\mathcal{V}_1 = \kappa x \begin{pmatrix} -1 & -1 \\ 1 & 1 \end{pmatrix} \tag{21}$$

and

$$V_2 = \varepsilon^2 \frac{\partial}{\partial v} \begin{pmatrix} \langle x\rangle & 0 \\ 0 & \langle x\rangle - 1 \end{pmatrix}, \tag{22}$$

where we have redefined the position coordinate such that its origin coincides with the steady-state value $\langle x\rangle \approx E_R$ [see equation (13)]. Equation (19) resembles the time-dependent Schrödinger equation, but without the imaginary i since it describes a classical and not a quantum system. The 'Hamiltonian operator' $\mathcal{H}_0$ gives the free, decoupled evolution of the independent oscillator and SET systems, while the operator $\mathcal{V} = \mathcal{V}_1 + \mathcal{V}_2$ describes the interaction between the two systems with $\mathcal{V}_1$ giving the dependence of the SET tunnelling rates on the oscillator position and $\mathcal{V}_2$ giving the SET island number dependence of the electrostatic force acting on the oscillator.

Given the resemblance of equation (19) to the Schrödinger equation, we can consider applying approximation schemes that have been developed in quantum mechanics. We shall use a method developed for open quantum systems which is sometimes called the 'self-consistent Born approximation' (SCBA). A system is open when it is coupled to another system with an infinite number of degrees of freedom. The latter, infinite system is commonly termed the 'environment' or 'reservoir' and the approximation method seeks to derive simpler, effective equations of motion for the finite system alone where the environment degrees of freedom have been integrated out. In our case, the finite system of interest is the mechanical resonator

modelled as a harmonic oscillator, while the environment comprises the tunnelling electrons in the SET. Applying the SCBA as described in section 3.1 of [46], we obtain the following approximate effective equation of motion for the probability distribution $P_{HO}(x,v,t)$ of the oscillator:

$$\frac{\partial \mathcal{P}(x,v,t)_{HO}}{\partial t} = \mathcal{H}_{HO} P_{HO}(x,v,t)$$
$$+ \exp(\mathcal{H}_{HO}t) \mathrm{Tr}_{SET}[\mathcal{V}(t)\mathcal{P}_{SET}(0)] \exp(-\mathcal{H}_{HO}t) P_{HO}(x,v,t)$$
$$- \int_0^t dt' \exp(\mathcal{H}_{HO}t)$$
$$\mathrm{Tr}_{SET}[\mathcal{V}(t)\mathcal{P}_{SET}(0)] \, \mathrm{Tr}_{SET}[\mathcal{V}(t')\mathcal{P}_{SET}(0)]$$
$$\exp(-\mathcal{H}_{HO}t) P_{HO}(x,v,t)$$
$$+ \int_0^t dt' \exp(\mathcal{H}_{HO}t) \, \mathrm{Tr}_{SET}[\mathcal{V}(t)\mathcal{V}(t')\mathcal{P}_{SET}(0)]$$
$$\exp(-\mathcal{H}_{HO}t) P_{HO}(x,v,t), \tag{23}$$

where $\mathcal{H}_{HO} = \varepsilon^2 x(\partial/\partial v) - v(\partial/\partial x)$ is the Hamiltonian operator for the free harmonic oscillator and $\mathcal{V}(t) = \exp(-\mathcal{H}_0 t)\mathcal{V}\exp(+\mathcal{H}_0 t)$ is in the interaction picture. The initial, $t = 0$ probability distribution is assumed to be a product state: $\mathcal{P}(0) = P_{HO}(x,v,0)\mathcal{P}_{SET}(0)$, where $\mathcal{P}_{SET}(0) = \begin{pmatrix} P_N(0) \\ P_{N+1}(0) \end{pmatrix}$.

The influence of the SET on the oscillator is contained in the 'trace' terms, such as $\mathrm{Tr}_{SET}[\mathcal{V}(t)P_{SET}(0)] = \sum_{\alpha=1}^{2} \sum_{\beta=1}^{2} \mathcal{V}_{\alpha\beta}(t)\mathcal{P}_{SET\beta}(0)$. All such terms in (23) and their integrals with respect to t' can be evaluated analytically. The resulting explicit expression for (23) is rather complicated, involving t-independent terms, t-dependent decaying terms of the form e^{-t}, as well as decaying oscillatory terms of the form $e^{-t}\cos(\varepsilon t)$ and $e^{-t}\sin(\varepsilon t)$. The terms also depend on the initial state $\mathcal{P}_{SET}(0)$ of the SET. However, if $\varepsilon << 1$, then we can neglect all decaying terms involving e^{-t} since, on timescales of order the mechanical period and longer, $t \gtrsim \varepsilon^{-1}$, such terms have a negligible effect on the oscillator dynamics. Furthermore, the dependence on the initial state of the SET drops out. Neglecting the time-dependent decaying terms is usually called the 'Markov' approximation, while the combined steps of the SCBA and Markov approximation are often simply called the 'Born-Markov' approximation. As a result, we obtain the following much simpler effective equation of motion for the oscillator:

$$\frac{\partial P}{\partial t} = \left[\varepsilon^2 x \frac{\partial}{\partial v} - v \frac{\partial}{\partial x} + \kappa \varepsilon^2 \frac{\partial}{\partial v}(v - x) \right.$$
$$\left. + \varepsilon^4 \langle P\rangle_N \langle P\rangle_{N+1} \frac{\partial}{\partial v}\left(\frac{\partial}{\partial v} + \frac{\partial}{\partial x}\right) \right] P, \tag{24}$$

where $\langle P\rangle_N$ and $\langle P\rangle_{N+1}(= 1 - \langle P\rangle_N \approx E_R)$ are the steady state SET island electron number probabilities [see equation (13)] and we have dropped the 'HO' subscript on the oscillator probability distribution $P(x,v,t)$ for

notational convenience. Expressing (24) in terms of dimensionful coordinates, we obtain

$$\frac{\partial P}{\partial t} = \left[\omega_R^2 x \frac{\partial}{\partial v} - v \frac{\partial}{\partial x} + \gamma_{\text{SET}} \frac{\partial}{\partial v} v + \frac{\gamma_{\text{SET}} k_B T_{\text{SET}}}{m} \frac{\partial^2}{\partial v^2} \right] P, \tag{25}$$

where recall the renormalized oscillator frequency is $\omega_R = \sqrt{1 - \kappa}\, \omega$, the damping rate is

$$\gamma_{\text{SET}} = \kappa \varepsilon \omega \tag{26}$$

and the effective SET temperature T_{SET} is defined in (17).

Equation (25), which goes by the name 'Klein-Kramers' or 'Fokker-Planck' equation [47], describes the brownian motion of a harmonic oscillator interacting with a thermal bath; the oscillator experiences a damping force due to the SET [the third term on the right-hand-side of equation (25)] with quality factor $Q_{\text{SET}} = \omega/\gamma_{\text{SET}} = 1/(\kappa \varepsilon)$ (since $\kappa << 1$, the renormalized frequency can be replaced by the unrenormalized frequency in the definition of the quality factor) and an accompanying Gaussian distributed thermal fluctuating force [the fourth term on the right-hand-side of (25), called the 'diffusion' term]. The $\partial^2 P/\partial x \partial v$ term in equation (24) (called the 'anomalous diffusion' term in [45]) has been neglected because it is of order ε smaller than the diffusion term when time is expressed in units of the oscillator period; it should have only a small effect on timescales of order the mechanical period or longer. The first moment of the fluctuating force which gives rise to the diffusion term vanishes, $\langle F(t) \rangle = 0$, while its second moment is

$$\langle F(t) F(t') \rangle = \frac{2 \gamma_{\text{SET}} k_B T_{\text{SET}}}{m} \delta(t - t'). \tag{27}$$

The delta function in equation (27) signifies that the kicks inflicted on the oscillator by the SET are uncorrelated, no matter how small is the distinct time interval separating the kicks. This amounts to taking the limit $\tau_{\text{tunnel}} \to 0$, which is justified provided $\tau_{\text{tunnel}} << 2\pi/\omega$ (equivalently $\varepsilon << 1$) and we are interested only in the oscillator dynamics on timescales $t \gtrsim 2\pi/\omega$ as discussed above. The condition $\varepsilon << 1$ appears necessary for the oscillator to perceive the SET as a thermal bath; if the condition did not hold, then it would be possible to infer from the oscillator dynamics that it was coupled to a tunnelling electron device and not to a many degree-of-freedom system in a state of thermal equilibrium.

The second and third terms on the right-hand-side of equation (23) involving traces of single interaction potential operators $\mathcal{V}(t)$ vanish by virtue of the Markov approximation and also the fact that the position coordinate was originally redefined such that the origin coincides with the steady-state value. The damping and diffusion terms in equation (24) arise from the fourth term on the right-hand-side of equation (23) involving the trace of the interaction potential operator product $\mathcal{V}(t)\mathcal{V}(t')$. More specifically, only products of the form $\mathcal{V}_2(t)\mathcal{V}_1(t')$ and $\mathcal{V}_2(t)\mathcal{V}_2(t')$ [see definitions (21) and (22)] give non-zero contributions, with the damping and frequency renormalization terms arising from the first product and the diffusion and anomalous diffusion terms arising from the second product. Thus, the effective thermal bath description for the SET crucially requires one to take into account not only the influence of the SET on the oscillator ($\mathcal{V}_2$), but also the influence of the oscillator on the SET as well ($\mathcal{V}_1$).

In our analysis of the coupled SET-oscillator dynamics, we have neglected the coupling between the oscillator and its external thermal bath. Incorporating the external bath into the equations of motion is straightforward: we just add the term

$$\gamma_{\text{ext}} \frac{\partial (v P)}{\partial v} + \frac{\gamma_{\text{ext}} k_B T_{\text{ext}}}{m} \frac{\partial^2 P}{\partial v^2} \tag{28}$$

to the above Fokker-Planck equation (25), where we assume again for simplicity that the influence of the external bath on the oscillator is uncorrelated and memoryless. The damping and fluctuating force terms due to the SET and external bath can be combined respectively to yield a single damping term with effective quality factor $Q_{\text{eff}}^{-1} = Q_{\text{SET}}^{-1} + Q_{\text{ext}}^{-1}$ and a single fluctuating force term with effective temperature

$$T_{\text{eff}} = Q_{\text{eff}} \left(\frac{T_{\text{SET}}}{Q_{\text{SET}}} + \frac{T_{\text{ext}}}{Q_{\text{ext}}} \right). \tag{29}$$

Summarizing so far, we have learned that provided the mechanical oscillator and SET are weakly coupled ($\kappa << 1$) and, furthermore, provided the SET dynamics occurs on much shorter timescales than the oscillator dynamics ($\varepsilon << 1$), then the oscillator behaves effectively as if it is in contact with a thermal bath, with figure 7 being replaced by the much simpler figure 10.

For typical SET device parameters and micron-scale resonators with frequencies of the order of a few megahertz, separated by a resonator-island electrode gap of about 0.1 μm, one obtains effective SET temperatures of around 1K and effective SET quality factors ranging from around 10^4 down to 10^2 as the gate voltage increases from 1V up to 10V [23]. External temperatures and quality factors for micron-scale resonators are of the order 100 mK and $10^4 - 10^5$, respectively, so that it should be possible to measure the effects of the SET temperature and quality factor on the mechanical resonator. Experiments are underway in Keith Schwab's group to probe the coupled dynamics of the SET and mechanical resonator [48]. They
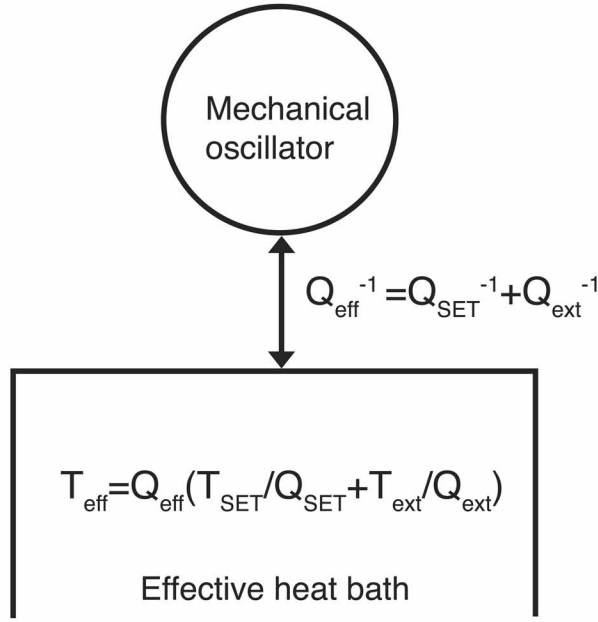
Figure 10. Scheme of the SET-oscillator system under the conditions of weak coupling and wide separation of dynamic timescales between the SET and oscillator. The oscillator undergoes thermal brownian motion, behaving as if in contact with a thermal bath at temperature $T_{\mathrm{eff}} = Q_{\mathrm{eff}}(T_{\mathrm{SET}}/Q_{\mathrm{SET}} + T_{\mathrm{ext}}/Q_{\mathrm{ext}})$, where $Q_{\mathrm{eff}}^{-1} = Q_{\mathrm{SET}}^{-1} + Q_{\mathrm{ext}}^{-1}$.

have seen evidence in several devices that the SET behaves as an effective bath, heating the resonator and causing damping which increases with gate voltage. This is the first time that the back action of electronic shot noise on a nanomechanical resonator has been observed. Note, however, that they work with superconducting SETs (SSETs), where tunnelling processes involve Cooper pairs as well, so that the above formulae for T_{SET} and Q_{SET} do not apply. It is important then to also analyze the SSET-mechanical resonator coupled dynamics [49,50].

4. Effective equilibrium dynamics of other NEMS

In this section, we consider the effective equilibrium dynamics of some of the other NEM devices described in section 2. One of the first theoretical investigations to establish that a far-from-equilibrium electronic device can behave like an effective thermal bath was conducted by Dima Mozyrsky and Ivar Martin at Los Alamos [22]. They considered a model device comprising a single, electrical tunnel junction with tunnelling rates depending on the position coordinate of a nearby mechanical oscillator, as illustrated in figure 11.

Solving the quantum Schrödinger equation for the coupled, tunnelling electrons-oscillator system, they found

under the conditions of weak coupling and Markovian approximation that the oscillator behaves effectively as if it is in contact with a thermal bath, with the tunnel junction characterized by a damping rate and a temperature given by

$$k_{\mathrm{B}} T_{\mathrm{TJ}} = eV/2, \tag{30}$$

where V is the voltage applied across the tunnel electrodes.

Thus, despite the differences between the tunnel junction and SET (two tunnel junctions in series with gated central island), both can behave effectively as a heat bath. In fact, the similarity in their statistical properties goes further. It turns out that their respective temperature expressions (17) and (30) can be commonly equated to the ensemble-averaged energy gained by an electron due to tunnelling across a junction [23]. For the tunnel junction, the averaged energy gained is $eV/2$, assuming zero electron temperature and constant density of states in the electrodes, as well as energy-independent tunnelling matrix [22,31]. For the SET, with the same asumptions the average energy gained by a tunnelling electron is $(E_R/2)\langle P \rangle_N + (E_L/2)\langle P \rangle_{N+1} \approx eV_{\mathrm{ds}}\langle P \rangle_N \langle P \rangle_{N+1}$ for $\kappa << 1$, where we have used equations (9), (10) and (13).

While the mechanically compliant tunnel electrode illustrated in figure 2 closely resembles the just-considered model tunnel junction (figure 11), there is a difference in that the tunnelling electrons will give a momentum recoil to the mechanically compliant electrode, which is of course absent for the fixed electrode. To our knowledge, there has yet to be a comprehensive analysis of the coupled dynamics of tunnelling electrons and mechanically compliant electrode, including the effects of momentum recoil. Nevertheless, one might expect that under the appropriate conditions of weak coupling and wide separation of dynamical timescales between the mechanical and electronic degrees of freedom, the effective thermal bath description again arises.

As mentioned in section 2, the electronic and mechanical dynamics are strongly coupled in the classical charge shuttle (figure 6); in order for a current to flow, the nanomechanical island electrode must shuttle charge between the drain and source electrodes, so that the dynamical timescales of the mechanical and electronic degrees of freedom are comparable. Because it is not possible to have a wide separation of timescales, it is unlikely that there is a regime in which the electron tunnelling dynamics is effectively that of a thermal bath, as perceived by the mechanical shuttle. The only possibility of separating the timescales is to make the drain-source electrode gap smaller than the electron tunnelling length (so that a tunnelling current can flow without the nanomechanical island electrode having to move from drain to source electrode), likely an unrealisable regime for nanoscale mechanical resonators that must fit in the gap.
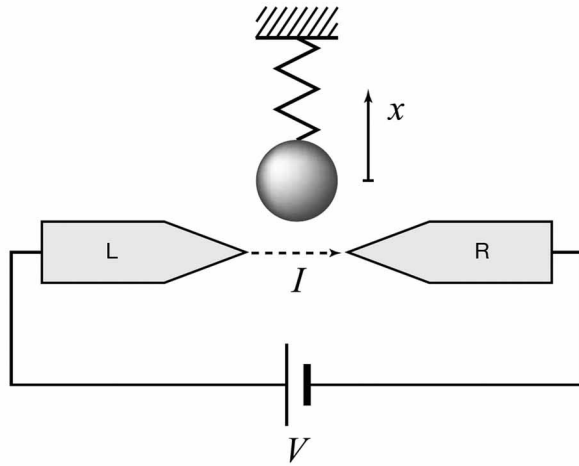
Figure 11. Oscillator coupled to an electrical tunnel junction [22]. As a result of an applied voltage V, electrons will tunnel from the right (R) to left (L) electrode, with tunnel rates depending on the position x of a nearby mechanical oscillator. The electromechanical coupling can be achieved by putting a net non-zero charge (or voltage) on a metallized mechanical oscillator.

Thus, provided the electron dynamics is stochastic, the electromechanical coupling strength is weak and the mechanical dynamics is much slower than the electron dynamics, the above examples suggest that the electronic device can be effectively replaced by a thermal bath for the reduced dynamics of the coupled mechanical resonator, so that figure 7 can be replaced by figure 10 (but now refering to a generic NEMS). How might one go about providing a proof of this conjecture for a general class of electromechanical systems? A possible direction is suggested by the Born-Markov approximation method applied to the SET-resonator system in section 3.3. In fact, the derivation of the Fokker-Planck equation (that ensures the effective thermal bath description) does not depend on the detailed form of the matrices appearing in the definitions (21) and (22) of the interaction operators $\mathcal{V}_1$ and $\mathcal{V}_2$, respectively; the derivation of the Fokker-Planck equation should carry through for additional and different types of tunnelling process, e.g. for a superconducting SET [50]. Of course, the detailed expressions for the renormalized frequency, damping constant and temperature will differ from one device to another. The important necessary steps that lead to the Fokker-Planck equation are the second order expansion in the interaction operator $\mathcal{V}$ (Born approximation – requires weak coupling) and the neglect of time-dependent decaying terms in the electron dynamics (Markov approximation – requires fast electron dynamics as compared with mechanical oscillator period). A suitable starting point for a general proof would be to write down a

Boltzmann/master equation involving a probability density function $P_{\{k\}}(x,v,t)$ where (x,v) are the oscillator's classical position/velocity coordinates and $\{k\}$ denotes some appropriate choice of electronic coordinates. The general interaction operator $\mathcal{V}$ should involve both position and velocity (to account for momentum recoil) dependent terms. The proof would then involve applying the Born-Markov approximation to this master equation, recovering the Fokker-Planck equation. An important proviso, however, is that there is no guarantee that the electronic device can necessarily damp the oscillator. The tunnelling dynamics may be such that it is more likely for an electron to give rather than to take energy from an oscillator, resulting in unstable coupled dynamics. This instability manifests itself through 'negative damping' and 'negative temperature' coefficients in the Fokker-Planck equation. Such an instability occurs in the case of the superconducting SET for certain ranges of gate and drain-source voltage [49,50].

A proof of the effective thermal bath description along the above lines has recently been demonstrated by Aashish Clerk at McGill University [41]. He gives a quantum treatment, with the electronic device modelled as a generic linear response detector of the quantum oscillator's position (essentially the quantum version of figure 7), to which it is weakly coupled. The proof is in part a generalization of Mozyrsky and Martin's analysis of the tunnel junction [22]. However, as described above, when the coupled dynamics under consideration is classical it should be possible to give a similar proof within the framework of classical master equations. Indeed, in Mozyrsky and Martin's tunnel junction analysis, the condition $eV \gg \hbar\omega$ is assumed, which from equation (30) amounts to taking the classical limit $k_B T_{TJ} \gg \hbar\omega$ for the oscillator. Certainly, a classical derivation of the effective thermal bath description for NEMS avoids having to simultaneously deal with the complicating (but fascinating) issue of how classical dynamics arises by approximation from quantum dynamics.

5. Conclusions

We have presented a brief overview of the field of NEMS research, with an emphasis on the classical effective dynamics of a nanomechanical resonator due to its interaction with a tunnelling electron system. Under the conditions of weak coupling and the characteristic mechanical dynamics occuring on much longer timescales than the tunnelling electron dynamics, the electron system can behave effectively as a heat bath, causing the resonator to undergo thermal brownian motion.

As they have been stated, the conditions for the resonator to perceive the electronic system as a thermal bath are rather general. It is natural therefore to wonder

whether there are other (semi)classical examples involving (not necessarily nanoscale) mechanical oscillators coupled to (not necessarily electronic) far from equilibrium systems with many degrees of freedom, such that the oscillator undergoes effective thermal brownian motion. Many such examples have in fact been considered. One example is laser Doppler cooling of a harmonically trapped ion [51,52]. The laser is tuned below the atomic resonance, so that the Doppler shift makes it more likely for the atom to absorb a photon with momentum oppositely directed to that of the atom than in the same direction, resulting in damping of the atom's motion. Despite the fact that the laser radiation field is obviously not a thermal equilibrium state, nevertheless under certain weak coupling and wide timescale separation conditions, the atom's dynamics is described by a Fokker-Planck equation [53], with effective temperature much lower than the ambient temperature: the laser cools the trapped ion. Another, recently considered macroscopic oscillator example [54] involves placing a sphere (ping-pong ball) in an upward gas-flow. It was found that the sphere behaves effectively as a harmonic oscillator undergoing thermal brownian motion, despite the far-from-equilibrium, turbulent state of the gas molecules. A derivation of this behaviour might start with a Boltzmann equation for a single massive particle undergoing collisions with a dilute gas of small mass particles, and then identifying the relevant small dimensionless coupling and timescale parameters for a subsequent series expansion of the Boltzmann equation. However, the recovery of a Fokker-Planck equation is not straightforward, owing to the relevance of the non-trivial turbulent gas dynamics for the effective dynamics of the oscillator. Yet another, related macroscopic example involves immersing a torsion oscillator in a far-from-equilibrium, vibration-fluidized granular medium [55–57]. Again, the granular medium was found to behave effectively as a thermal bath, with the oscillator undergoing thermal brownian motion.

Returning to the subject of NEMS, there are many aspects of their dynamical behaviour still to be understood. In the strong coupling regime (e.g. $\kappa \gtrsim 1$ in the case of the SET-oscillator system), little is known in general about the effective dynamics of the oscillator and also how the coupled dynamics manifests itself in the effective behaviour of the electronic system (e.g. current, current noise, etc.). Furthermore, little is known in general about the quantum dynamics of NEMS and how (semi)classical dynamics arises as a result of dephasing within the electronic system, as well as due to the external environment of the nanomechanical resonator.

Acknowledgments

References

[1] M.L. Roukes, Sci. Am. **285** 48 (2001).

[2] M.L. Roukes, Phys. World **14** 25 (2001).

[3] M.L. Roukes, in *Techical Digest 2000 Solid-State Sensor and Actuator Workshop* (Tranducer Research Foundation, Cleveland, 2000); lanl e-print cond-mat/0008187.

[4] A.N. Cleland, *Foundations of Nanomechanics* (Springer, Heidelberg, 2002).

[5] R.H. Blick, A. Erbe, L. Pescini, *et al.*, J. Phys.: Condens. Matter **14** R905 (2002).

[6] M.P. Blencowe, Phys. Rep. **395** 159 (2004).

[7] X.M. H. Huang, C.A. Zorman, M. Mehregany, *et al.*, Nature **421** 496 (2003).

[8] A.N. Cleland and M.R. Geller, Phys. Rev. Lett. **93** 070501 (2004).

[9] R. Knobel, and A.N. Cleland, Nature **424** 291 (2003).

[10] J.A. Sidles, J.L Garbini, K.J. Bruland, *et al.*, Rev. Mod. Phys. **67** 249 (1995).

[11] D. Rugar, R. Budakian, H.J. Mamin, *et al.*, Nature **430** 329 (2004).

[12] P.C. Hammel, Nature **430** 300 (2004).

[13] B. Ilic, H.G. Craighead, S. Krylov, *et al.*, J. Appl. Phys. **95** 3694 (2004).

[14] K.L. Ekinci, X.M.H. Huang and M.L. Roukes, Appl. Phys. Lett **84** 4469 (2004).

[15] K.L. Ekinci, Y.T. Yang and M.L. Roukes, J. Appl. Phys. **95** 2682 (2004).

[16] M.P. Blencowe, Nature **424** 262 (2003).

[17] M.D. Lahaye, O. Buu, B. Camarota, *et al.*, Science **304** 74 (2004).

[18] M.P. Blencowe, Science **304** 56 (2004).

[19] D.V. Scheible and R.H. Blick, Appl. Phys. Lett. **84** 4632 (2004).

[20] V. Sazonova, Y. Yaish, H. Üstünel, *et al.*, Nature **431** 284 (2004).

[21] A.N. Cleland, Nature **431** 251 (2004).

[22] D. Mozyrsky and I. Martin, Phys. Rev. Lett. **89** 018301 (2002).

[23] A.D. Armour, M.P. Blencowe and Y. Zhang, Phys. Rev. B **69** 125313 (2004).

[24] J. Casas-Vázquez and D. Jou, Rep. Prog. Phys. **66** 1937 (2003).

[25] N.F. Schwab, A.N. Cleland, M.C. Cross *et al.*, Phys. Rev. B **52** 12911 (1995).

[26] M.F. Bocko, K.A. Stephenson and R.H. Koch, Phys. Rev. Lett. **61** 726 (1988).

[27] B. Yurke and G.P. Kochanski, Phys. Rev. B **41** 8184 (1990).

[28] C. Presilla, R. Onofrio and M.F. Bocko, Phys. Rev. B **43** 3735 (1992).

[29] R. Onofrio and C. Presilla, Europhys. Lett. **22** 333 (1993).

[30] A.A. Clerk and S.M. Girvin, Phys. Rev. B **70** 121303(R) (2004).

[31] A.Yu. Smirnov, L.G. Mourokh and N.J.M. Horing, Phys. Rev. B **67** 115312 (2002).

[32] Y. Xue and M.A. Ratner, Phys. Rev. B **70** 155408 (2004).

[33] G. Binnig and H. Rohrer, Rev. Mod. Phys. **59** 615 (1987).

[34] A.N. Cleland, J.S. Aldridge, D.C. Driscoll, *et al.*, Appl. Phys. Lett. **81** 1699 (2002).

[35] L.J. Challis, Contemp. Phys. **33** 111 (1992).

[36] S. Sapmaz, Ya.M. Blanter, L. Gurevich, *et al.*, Phys. Rev. B **67** 235414 (2003).

[37] R.I. Shekhter, Yu. Galperin, L.Y. Gorelik, *et al.*, J. Phys.: Condens. Matter **15** R441 (2003).

[38] F. Pistolesi, Phys. Rev. B **69** 245409 (2004).

[39] A.D. Armour, Phys. Rev. B **70** 165315 (2004).

[40] C. Flindt, T. Novotný and A.P. Jauho, Europhys. Lett. **69** 475 (2005).

[41] A.A. Clerk, Phys. Rev. B **70** 245306 (2004).

[42] F. Pistolesi and R. Fazio, Phy. Rev. Lett. **94** 036806 (2005).

[43] D.S. Lemons, *An Introduction to Stochastic Processes in Physics* (Johns Hopkins Press, Baltimore, 2002).

[44] M. Amman, R. Wilkens, E. Ben-Jacob, *et al.*, Phys. Rev. B **43** 1146 (1991).

[45] D.K. Ferry and S.M. Goodnick, *Transport in Nanostructures* (Cambridge University Press, Cambridge, 1997).

[46] J.P. Paz and W.H. Zurek, in *Coherent Atomic Matter Waves: Les Houches-Ecole d'Été de Physique Théorique*, Vol. 72, edited by R. Kaiser, C. Westbrook and F. David (Springer-Verlag, Berlin/Heidelberg, 2000); lanl e-print quant-ph/0010011.

[47] H. Risken, *The Fokker-Planck Equation* (Springer-Verlag, Berlin/Heidelberg, 1989).

[48] K. Schwab, personal communication (2004).

[49] A.A. Clerk, in preparation (2005).

[50] M.P. Blencowe, J. Imbers and A. D. Armour, in preparation (2005).

[51] W.D. Phillips, Rev. Mod. Phys. **70** 721 (1998).

[52] C.J. Foot, Contemp. Phys. **32** 369 (1991).

[53] J. Javanainen and S. Stenholm, Appl. Phys. **21** 283 (1980).

[54] R.P. Ojha, P.-A. Lemieux, P.K. Dixon, *et al.*, Nature **427** 521 (2004).

[55] G. D'Anna, P. Mayor, A. Barrat, *et al.*, Nature **424** 909 (2003).

[56] P. Umbanhowar, Nature **424** 886 (2003).

[57] A. Baldassarri, A. Barrat, G. D'Anna, *et al.*, lanl e-print cond-mat/0501488.

Miles Blencowe received his B.Sc. (1986) and Ph.D. (1989) degrees in theoretical physics at Imperial College. He subsequently held postdoctoral fellowships at the University of Cambridge (1989–1991), the University of Chicago (1991–1993) and the University of British Columbia (1993–1994). Following a senior research associate position at Imperial College (1994–1999), he moved to Dartmouth College where he is currently an associate professor in the Department of Physics and Astronomy. His research interests lie in the areas of mesoscopic physics, quantum information theory applied to solid state systems, and non-equilibrium statistical mechanics.